Pergamon

Engineering Failure Analysis, Vol. 4, No. 1, pp. 57–70, 1997

Printed in Great Britain
1350-6307/97 $17.00 + 0.00

PII:S1350-6307(96)00024-6

FAILURES OF CHAIN SYSTEMS

ALAN JAMES

Metallurgical and Corrosion Services Programme, MATTEK, CSIR, Private Bag X28, Auckland Park 2006, Republic of South Africa

(*Received* 29 *August* 1996)

Abstract—Chains are used for various purposes in a wide range of industries. This paper describes three case studies where a failure analysis was carried out on chains used in markedly different applications. The failure mechanisms emphasize the importance of operating the equipment within the original design parameters, and also that material integrity is fundamental to the operational life of a system. © 1997 Elsevier Science Ltd. All rights reserved.

1. INTRODUCTION

Chains are used in a variety of applications in engineering practice. In general, there are three basic types of system:

hoisting and securing chains
conveying and elevating chains
power transmission chains

The materials used can vary significantly and are specifically tailored for the application. For example, a conveying system in a bottling plant is basically a means to hygienically move items from A to B under relatively low loads, and, therefore, a system of polypropylene "table-top" links connected by stainless steel pins is employed. On the other hand, an anchor chain for a marine vessel needs to be extremely strong: therefore, large-gauge steel chain links are necessary to withstand the static and dynamic loads imposed on the system.

A chain is normally used as a simple, low-cost means of transmitting motion or absorbing relative motion between two bodies, and in the simplest form is a series of interconnecting links of finite length. More complicated systems employing multiple leaf plates and pins, or a combination of rollers, bushes, plates and pins, are widely used. However, the more complicated the mechanical system, in general, the more susceptible it is to operational changes and the more maintenance is required to ensure the system is in good working order.

The purpose of this paper is to highlight typical (or atypical) problems experienced by three chain systems used in widely different applications. The operating environments of the chain systems include a furnace hearth, a drilling rig for rock boring, and, finally, a dragline crane used for removing overburden.

2. CASE STUDY 1: FAILURE OF SCRAPER LINKS FROM A FURNACE CONVEYOR CHAIN

2.1. *Background*

This case study describes the failure analysis of two scraper links which had fractured in service. The links form part of a conveyor scraper chain system in the hearth of a furnace, and are used to remove debris which is normally at a temperature below 250 °C. The scraper chain system had been in operation for approximately 5 years. The links are manufactured from austenitic manganese steel castings to ASTM A128 Grade C.

2.2. *Failure analysis*

The links had fractured near one of the scraper flanges, resulting in the detachment of one locating arm (Fig. 1). The fracture surfaces were characteristic of brittle failure (Fig. 2). One of the fractured links showed extensive blue colouration due to heat oxidation.

A sample cut from one of the scraper links was subjected to chemical analysis. The results are presented in Table 1.

One of the fracture surfaces was examined using scanning electron microscopy. There was evidence of interdendritic cracking and porosity (Fig. 3), with limited surface oxidation. The fracture surface showing the heat discolouration was also examined, and this showed extensive oxidation and characteristic loosely adhering particles.

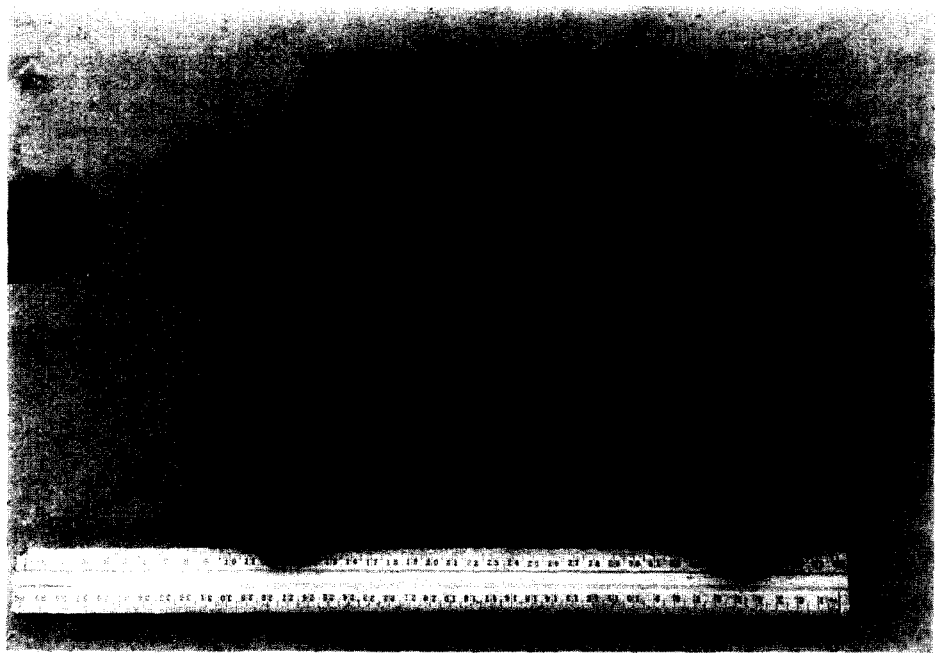

Fig. 1. General view of the fractured scraper chain link.

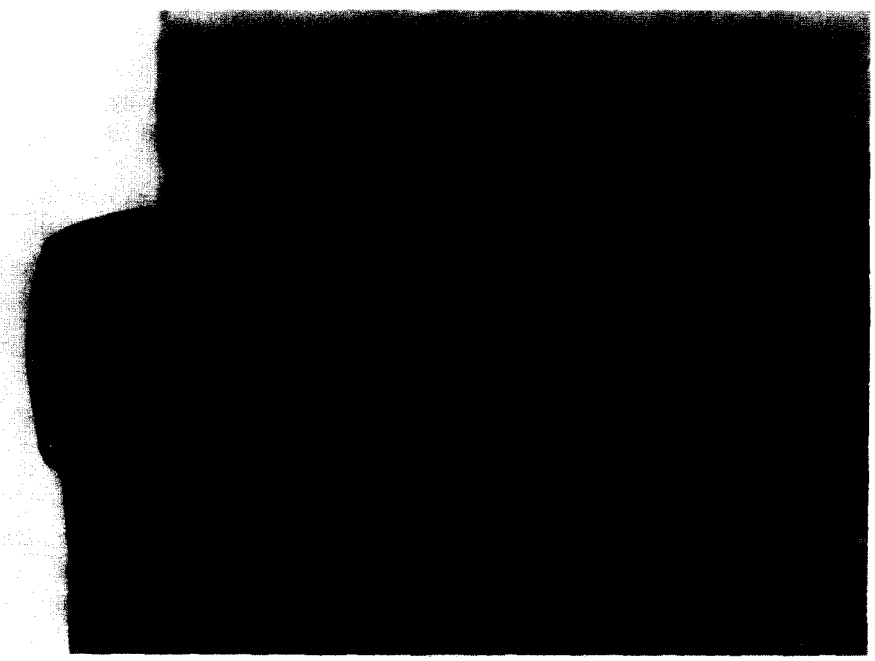

Fig. 2. Link fracture surface, showing features characteristic of brittle failure.

Table 1. Chemical analysis of one scraper chain link: composition in wt %

	C	Mn	S	P	Si	Cr	Mo	Ni	Fe
Link	1.26	12.30	0.005	0.063	1.61	1.11	0.02	0.14	Balance
ASTM A128 Grade C	1.05–1.35	11.50–14.00	—	≤0.07	≤1.00	1.50–2.50	—	—	Balance

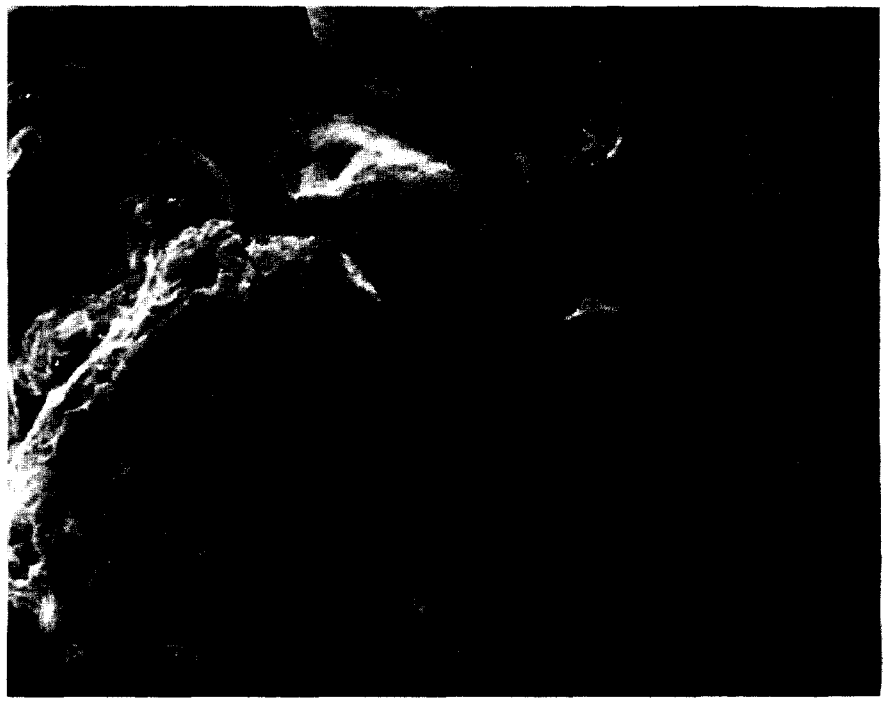

Fig. 3. Scanning electron fractograph showing interdendritic cracking and porosity. × 730.

A section was cut across one of the surfaces and prepared for optical microscopy using standard metallographic procedures. Etching revealed that the fracture path predominantly followed a network of precipitated carbide at the austenite grain boundaries (Fig. 4). The carbide network is more

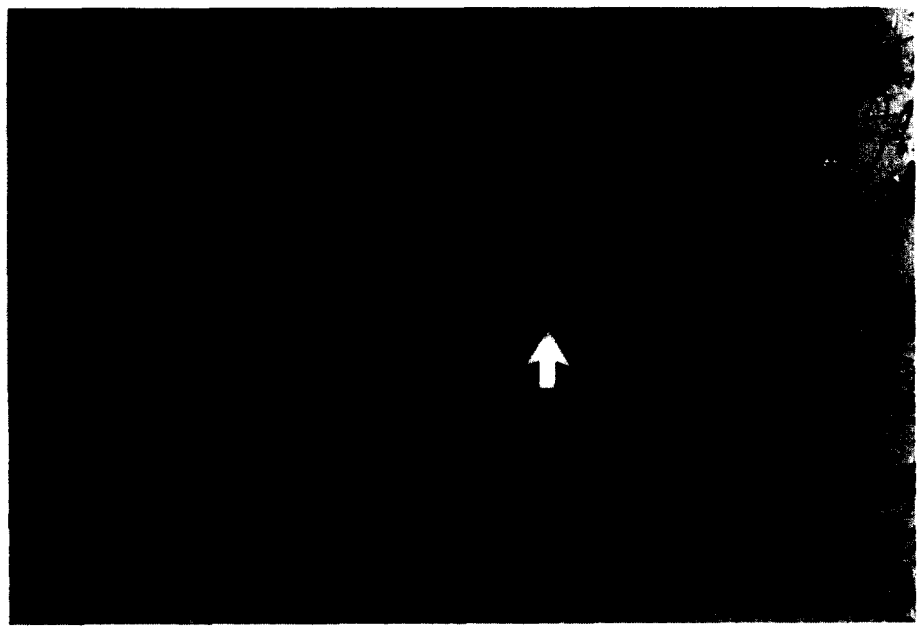

Fig. 4. Optical micrograph at the fracture surface, showing cracking following grain boundary carbide (arrowed). Etched in 2% nital. × 285.

Fig. 5. Partial decarburization and intergranular carbide network near the surface of the link. Etched in 2% nital. ×285.

clearly shown in Figs 5 and 6, which show, respectively, an area of partial decarburization adjacent to the outer surface of the link and an area from the centre of the link with carbides throughout the microstructure. No material or manufacturing defects were found, the level of interdendritic porosity being very small.

A sample cut from one of the links was heat treated in a laboratory air-circulating furnace for 1 h at 1120 °C, and subsequently cold water quenched. After suitable preparation, a section was examined using optical microscopy, revealing a completely austenitic microstructure (Fig. 7). In order to establish the temperature at which blue heat tinting occurs, a series of heat treatments was carried out on material at different temperatures in the laboratory furnace. It was found that the discolouration initiated at 400 °C.

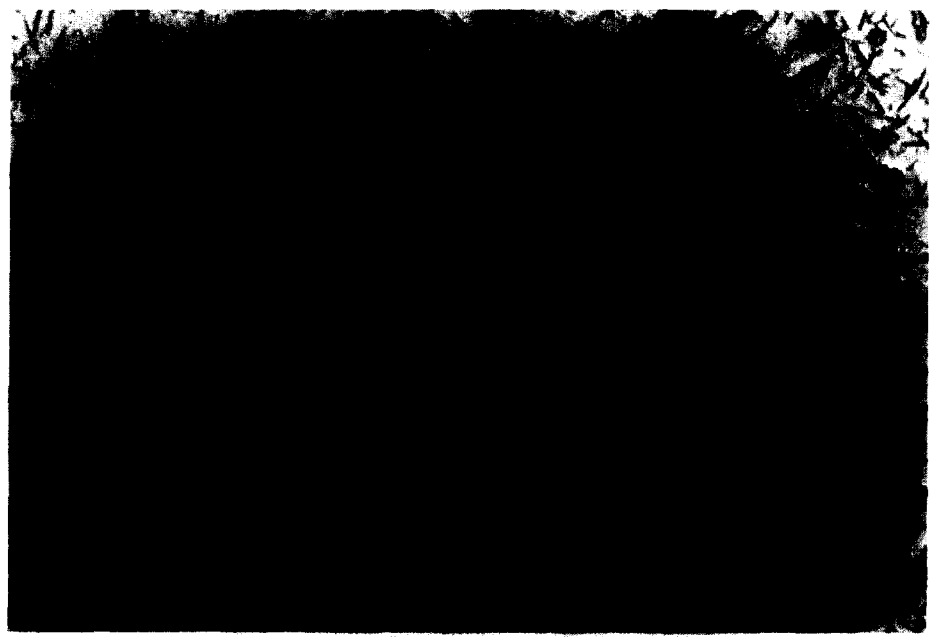

Fig. 6. General carbide precipitation at the centre of the link material. Etched in 2% nital. ×285.

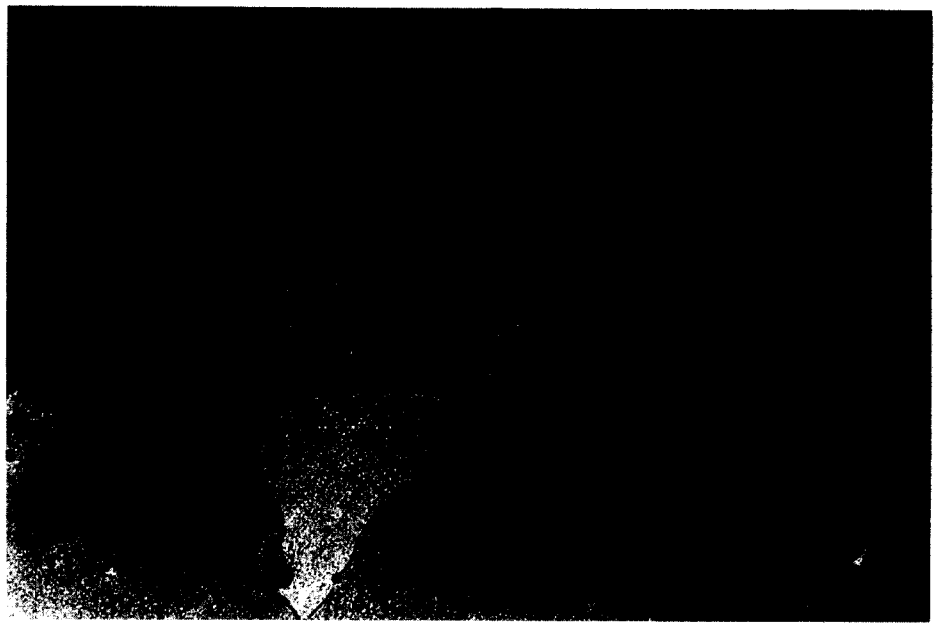

Fig. 7. The link material after reheating, showing a completely austenitic microstructure. Etched in 2% nital. ×285.

2.3. *Discussion*

Apart from a slightly low chromium content, the scraper chain links have been manufactured from an austenitic manganese steel similar to ASTM A128 Grade C. Fractographic examination and optical microscopy has established that failure has occurred in a brittle manner due to prolonged exposure to temperatures in excess of 300 °C and intermittent exposure at 400–450 °C.

Unlike structural steels, which become softer and more ductile when reheated in service, manganese steels become brittle when reheated sufficiently to induce carbide precipitation or some transformation of the austenite. Generally, manganese steels should not be heated above 260 °C unless such heating is followed by re-solution annealing and water quenching. Embrittlement is time-, temperature- and composition-dependent, as shown in Fig. 8. At 260 °C, transformation requires more than 10,000 h exposure, whereas at 350 °C the exposure period is little more than 100 h. The effect of manganese and carbon content on the embrittlement of manganese steels is illustrated in Fig. 9. Higher nominal manganese and lower carbon contents are more desirable for steels subjected to "high" operating temperatures.

The ASTM A128 Grade C austenitic manganese steel is ideal for wear resistance but should not be used above 260 °C. For slightly higher operating temperatures, molybdenum-bearing steels are

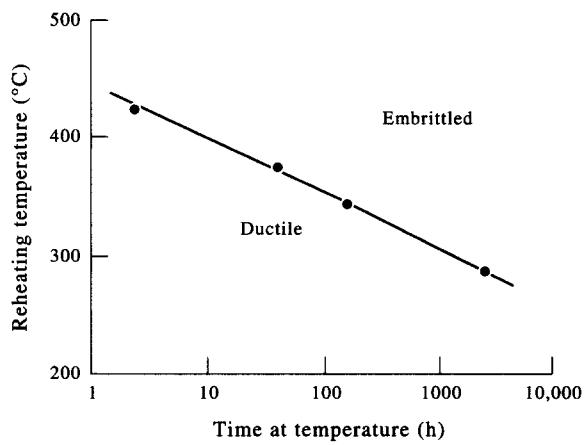

Fig. 8. Time–temperature relationship for the embrittlement of a 13% Mn– 1.2% C–0.5% Si steel (courtesy of ASM).

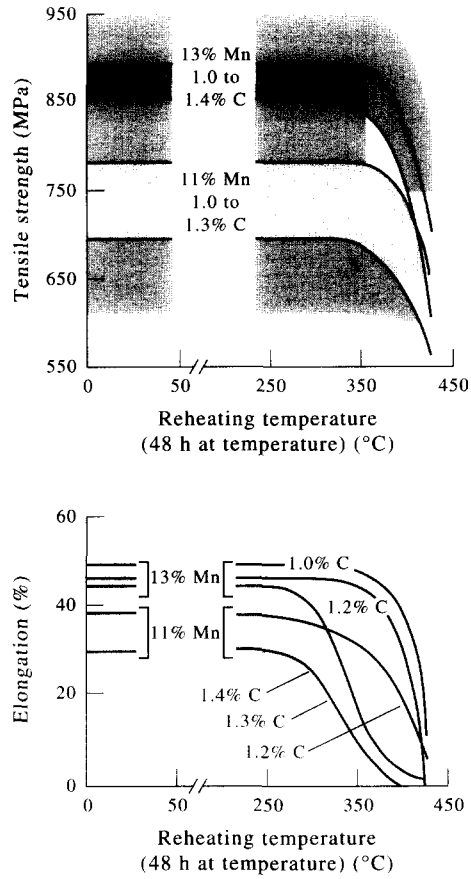

Fig. 9. Embrittlement from reheating manganese steels (courtesy of ASM).

often used. Molybdenum in solution suppresses carbide precipitation and reduces susceptibility to embrittlement, even when the austenite is exposed to temperatures above 275 °C [1].

2.4. *Conclusions and recommendations*

(1) The scraper chain links have fractured in a brittle manner due to prolonged exposure at excessive temperatures. The links have been manufactured from austenitic manganese steel similar to ASTM A128 Grade C, which is not recommended for use above 260 °C.
(2) The embrittlement can be eliminated by re-solution annealing: however, at these temperatures care should be taken to prevent distortion.
(3) If it is not possible to control the furnace hearth temperature, a more heat-resistant material, such as chromium–cobalt, should be used.

3. CASE STUDY 2: FAILURE OF A PULL-DOWN CHAIN FROM A DRILLING RIG

3.1. *Background*

This case study describes the failure analysis of leaf chain links which had fractured during service on a drilling rig. No details of the system were provided except that the chain had been in service for only 2 weeks prior to the failure. The chain is a multiple leaf linkage system consisting of 14 mm diameter locating pins connected in a $3 \times 2/1 \times 2 \times 2 \times 1$ configuration (Fig. 10).

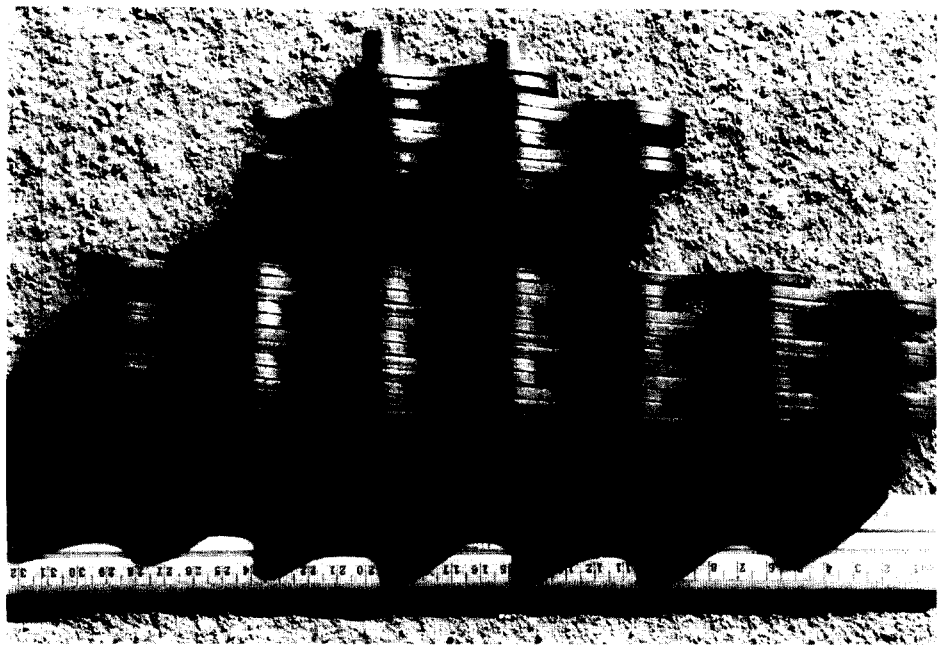

Fig. 10. Configuration of the pull-down leaf chain, compared to the sample of a fractured chain submitted for examination.

3.2. *Failure analysis*

The chain had failed locally, resulting in the fracture of numerous links and one side plate. Only two fractured links remained attached to the sample submitted for examination (Fig. 11). Both locating pins on the sample had been deformed.

Examination of the fracture surfaces revealed areas of fatigue on both links (Fig. 12). The fatigue cracking had originated from the surface of the locating hole and from the hole–side face intersection on one link, and from the hole surface on the other link. The areas of fatigue, compared to the total fracture areas of the links, were less than 5% on one link and less than 10% on the other, and had a fairly coarse texture.

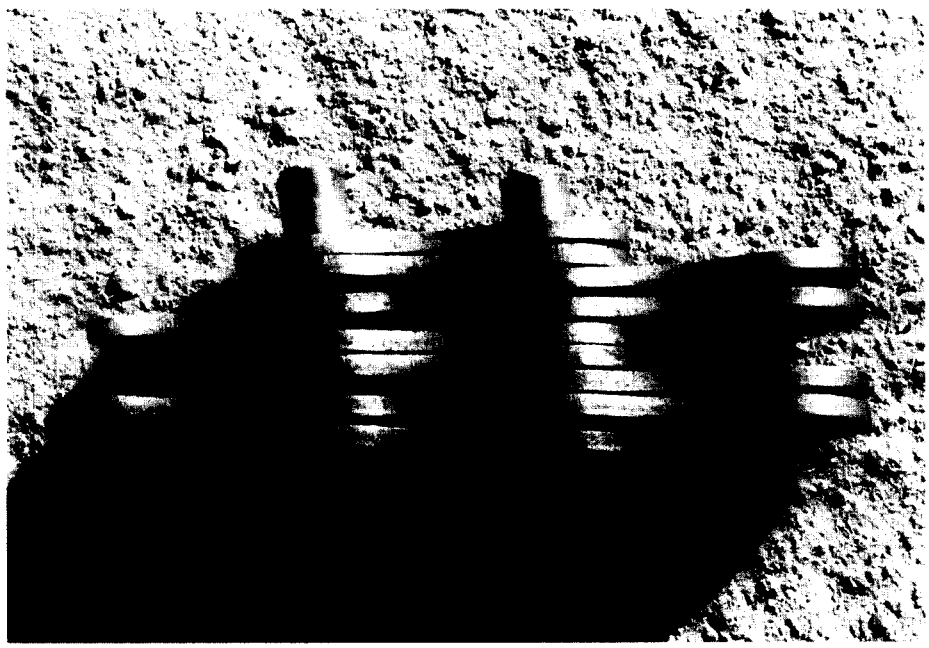

Fig. 11. Close-up view of the fractured sample of chain. Note the pin deformation.

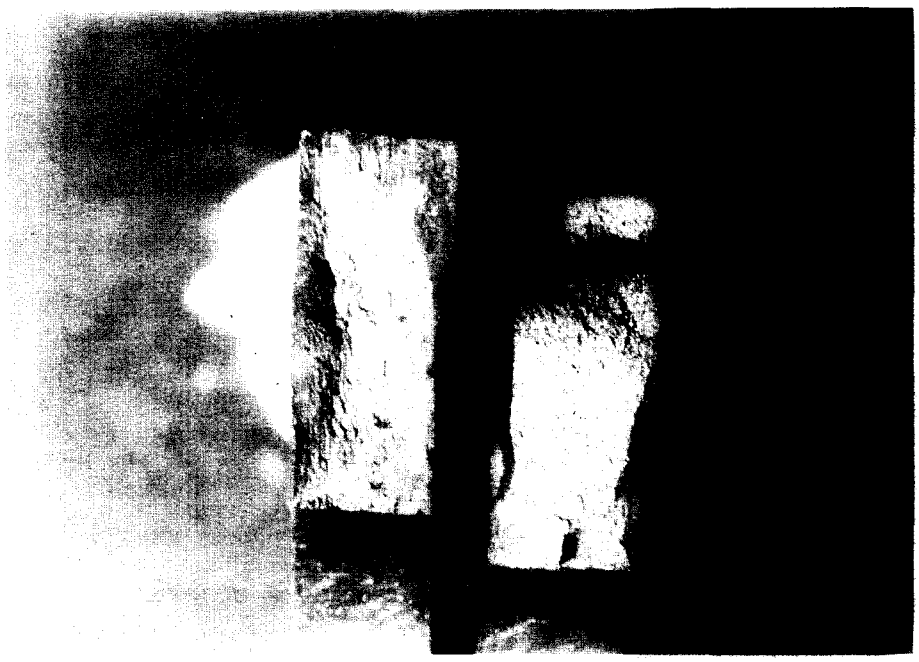

Fig. 12. Areas of fatigue on both fractured links.

A sample cut from one fractured link and from one deformed locating pin was subjected to chemical analysis. The results are presented in Table 2.

Scanning electron microscopy showed no clear evidence of fatigue striations due to degradation of the surfaces by rubbing.

A section was cut from a fractured link and from one of the deformed pins and prepared for microscopic examination using standard metallographic procedures. The microstructure of the link was indicative of tempered martensite: the pin had been carburized on the surface and had a tempered martensite core.

Hardness testing was carried out on a broken link and on the core of one pin, giving average figures of 445 and 417 HV, respectively.

3.3. *Discussion*

The pull-down chain has failed due to fatigue which has originated from the surface of the locating holes and from the hole–side face intersection. The area of fatigue crack propagation is relatively small, compared to the total fracture area, which is indicative of high operational stress. This may have been in the form of very high working loads or a combination of high loads and a sudden event such as dynamic loading. Clearly, the stress necessary to cause deformation of the locating pins would have been appreciable.

Multiple ligament chain link systems can experience problems if the loading is non-uniform or if the system is subjected to dynamic loading. In addition, adequate lubrication of such chain systems is very important to ensure that friction (and surface corrosion) is reduced as much as possible. Abnormal loading, directly from dynamics or indirectly from the increased power necessary to move the system due to frictional resistance, can induce degradation and failure of leaf chains.

Table 2. Chemical analysis of a link and pin: composition in wt %

	C	Mn	S	P	Si	Cr	Mo	Fe
Link	0.38	1.52	0.010	0.033	0.27	0.17	0.20	Balance
DIN Specification 36Mn5	0.32–0.40	1.20–1.50	⩽0.035	⩽0.035	0.15–0.35	0.30 maximum		Balance
Pin	0.15	0.83	0.015	0.015	0.22	1.14	0.24	Balance
DIN Specification 15CrMo5	0.13–0.17	0.80–1.10	⩽0.035	⩽0.035	0.15–0.35	1.00–1.30	0.20–0.40	Balance

3.4. *Conclusions and recommendations*

(1) The pull-down chain has failed by fatigue originating from the 14 mm diameter locating holes in the leaf links.
(2) The failure of the chain is due to excessive operational stresses.
(3) Consideration should be given to using a higher-strength chain, or at least control or redistribute the operating loads on the system.

4. CASE STUDY 3: FAILURE OF A FRACTURED DRAG-CHAIN LINK OFF A DRAGLINE CRANE

4.1. *Background*

This case study describes the failure analysis of a link from a drag-chain. Drag-chains are used as linkages at the buckets of dragline cranes (Fig. 13). Due to the nature of their use, the chains have to be very robust. Refurbishment repairs of chain links are common. The links are normally cast in sets of four or six, and are subsequently joined to form the chain.

The link in question had been weld repaired to build up abraded areas several months prior to the failure, but had only been in service for a short time. The repair was carried out manually by flux cored arc welding using a preheat temperature of 150 °C and a maximum interpass temperature of 300 °C, using templestick temperature monitoring. After welding, the profile was ground smooth, and the link subjected to magnetic particle inspection and visual examination.

4.2. *Failure analysis*

The chain link had fractured at two positions adjacent to the stud in the centre of the link (Fig. 14). One of the fracture surfaces showed a smooth, oval region adjacent to the outer extremity of the link (Fig. 15), covering an area of approximately 20% of the cross-sectional area at the point of fracture. This area was cleaned in a hexamethylene tetramine–hydrochloric acid solution which is specifically formulated to remove surface oxide but not chemically damage the underlying surface. Beach markings, characteristic of fatigue crack propagation, were clearly observed (Fig. 16).

The fracture surface was examined in more detail using a stereomicroscope. This revealed that the origin of failure corresponded to a subsurface shrinkage defect (Fig. 17). Several slag inclusions were also observed. The shrinkage defect was measured to be 14 mm from the surface of the link.

A sample cut from the chain link was subjected to chemical analysis. The results are presented in Table 3.

A cross-section was cut through the link approximately 10 mm from the fracture plane, and etched to highlight the weld passes making up the repair (Fig. 18). Measurements indicated that the weld overlay material thickness was up to 2 mm in depth, with that of the associated heat-affected zones being up to 7 mm in depth.

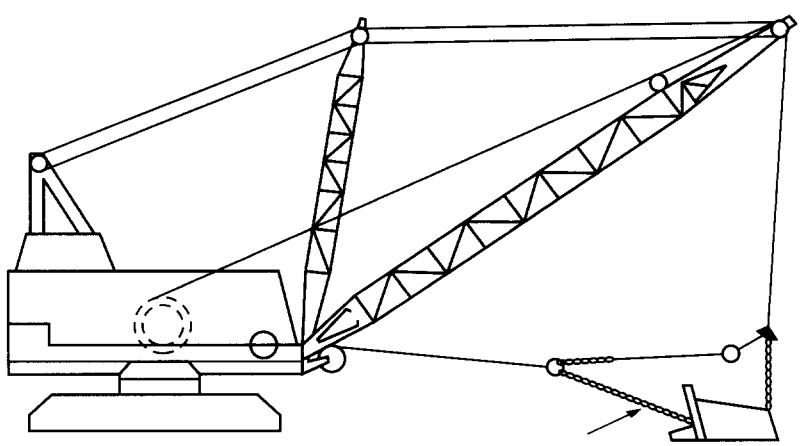

Fig. 13. Schematic diagram of a dragline crane showing the position of the drag-chain (arrowed).

Fig. 14. General view of the fractured drag-chain link (one-fifth of normal size).

Fig. 15. One of the fracture surfaces (as-received). Note the smooth area of cracking.

Fig. 16. Fracture surface after cleaning, showing distinct beach markings.

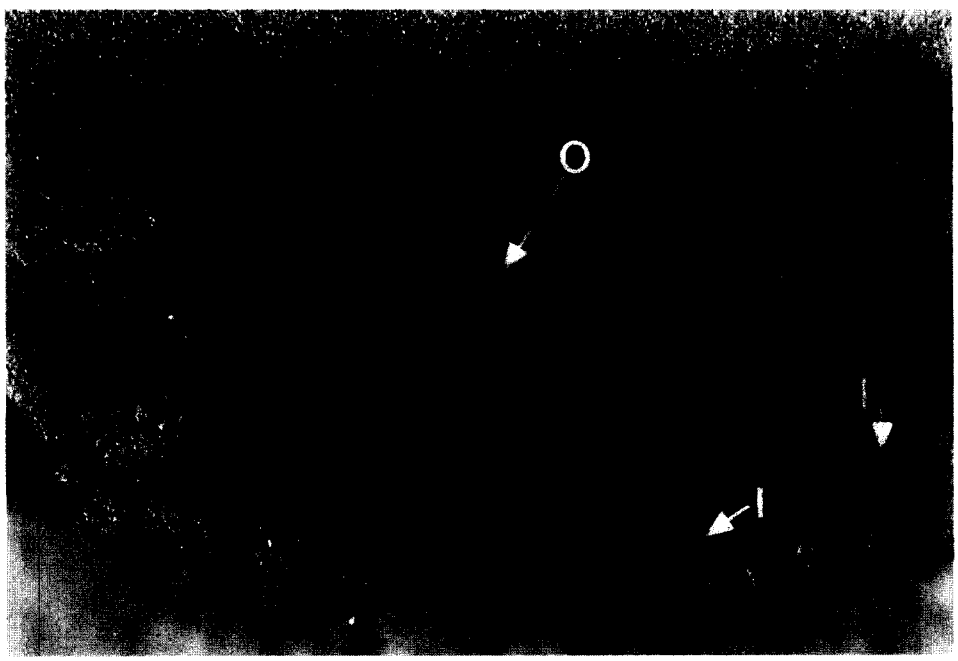

Fig. 17. Shrinkage defect at the origin of the fracture (O). Slag inclusions (I) are also evident on the fracture surface.

Table 3. Chemical analysis of the drag-chain link: composition in wt %

	Mn	S	P	Si	Cr	Mo	Ni	Cu	Al	V	Fe
0.23	1.11	0.012	0.02	0.63	1.06	0.31	0.84	0.10	0.052	0.011	Balance

Fig. 18. Transverse macrosection through the link, approximately 10 mm from the fracture plane. Etched in 2% nital. × 2 (approximately).

A section was cut from the area of fatigue fracture, and examined using scanning electron microscopy. The area around the fracture origin showed intergranular decohesion (Fig. 19). The smooth region of fracture previously observed during visual examination showed no evidence of any fatigue striations, the surface being damaged due to rubbing of the surfaces. A section of

Fig. 19. Scanning electron fractograph of the area near the origin, showing intergranular decohesion. × 1570.

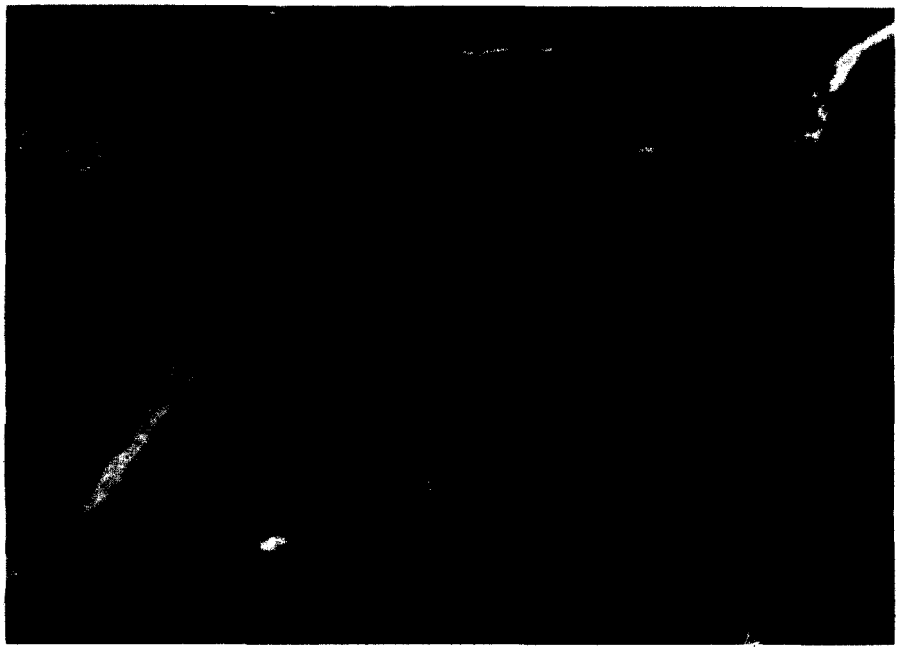

Fig. 20. Scanning electron fractograph of the final overload region of the fracture surface, showing brittle cleavage. × 1430.

material from the final overload region of the fracture surface showed features characteristic of brittle cleavage fracture (Fig. 20).

Optical microscopy was carried out on a longitudinal section of material cut adjacent to the origin of the fracture. The shallow weld overlay material was clearly observed (Fig. 21). The original cast material inboard of the weld heat-affected zone showed evidence of shrinkage cavities (Fig. 22).

Hardness testing was carried out using a Vickers type machine and a 10 kg load, giving average figures of 421 HV for the original link material and 294 HV for the weld material.

4.3. *Discussion*

The examination of the fractured drag-chain link has established that failure was due to fatigue and originated from subsurface shrinkage porosity. The defect is situated approximately 14 mm

Fig. 21. Optical micrograph across the weld overlay. Etched in 2% nital. × 85.

Fig. 22. Optical micrograph from the area of the original material inboard of the weld heat affected zone, showing shrinkage porosity. Etched in 2% nital. ×85.

from the surface of the link but does not coincide with the area of weld repair. The shrinkage porosity is, therefore, a residual defect from the original casting process.

From the nature of the beach markings on the fracture surface, it is very likely that the fatigue crack was present at the time of the repair, and was then "sealed", only to undergo further propagation prior to failure.

The intergranular mode of cracking at the fracture origin is rather unusual, but is probably associated with grain boundary segregation during cooling from the casting operation. Following crack initiation, the fatigue propagation progressed to form a roughly oval shaped crack until the link section could no longer withstand the applied loading experienced during normal dragline operations, and this resulted in final fast brittle failure.

The general microstructure of the link and weld overlay was found to be satisfactory. However, slag intrusions could prove deleterious to the integrity of the chain link. The link has been manufactured from a Cr–Mo–Ni alloy steel casting, and the hardness is typical. The lower hardness of the overlay is quite normal, as this is generally regarded as "sacrificial" material.

4.4. *Conclusions and recommendations*

(1) The drag-chain link failed by fatigue which originated from subsurface shrinkage porosity in the original cast material. Adequate non-destructive testing procedures should be carried out on the cast links in order to highlight potentially deleterious defects.
(2) The fatigue crack was probably present at the time of weld repair, and further propagation was necessary for the crack to achieve a critical size.

REFERENCE

1. *ASM Metals Handbook*, Vol. 3, 9th edn. American Society of Metals, Metals Park, OH, pp. 568–588.